



MiR-539 functions as a tumor suppressor in pancreatic cancer by targeting TWIST1

Haibo Yu^a, Ganglong Gao^c, Jing Cai^a, Hongliang Song^a, Zhongwu Ma^a, Xiaodan Jin^a, Wu Ji^{b,**}, Bujian Pan^{a,*}

^a Department of Hepatobiliary Surgery, Wenzhou Central Hospital, The Dingli Clinical Institute of Wenzhou Medical University, Wenzhou, Zhejiang 325000, PR China

^b Research Institute of General Surgery, Nanjing School of Clinical Medicine, Southern Medical University (Nanjing General Hospital of Nanjing Military Region), No.1023, South Shatai Road, Baiyun District, Guangzhou, 510515, Guangdong, PR China

^c Department of General Surgery, Shanghai fengxian district central hospital, Shanghai 201499, PR China

ARTICLE INFO

Keywords:

Pancreatic cancer
miR-539
TWIST1
Epithelial-mesenchymal transition

ABSTRACT

The dysregulation of microRNA (miRNA) expression has been highlighted in a variety of human malignant conditions with reports implicating a critical role in the process of tumor growth. The role of miR-539 in pancreatic cancer (PC) is yet to be fully elucidated, hence the aim of the current study was to investigate the effect of miR-539 expression in relation to a cohort of 52 PC specimens. The application of a real-time quantitative polymerase chain reaction (qRT-PCR) revealed a significantly down-regulated miR-539 level, which was accompanied by an increased TWIST1 expression in PC when compared with the controls. The *in vitro* experiment results demonstrated that the endogenous mimic of miR-539 significantly suppressed the growth of the xenograft tumors in PANC-1 cells, when compared to the delivery of the control miRNA and blank control. Meanwhile, the key epithelial-mesenchymal transition (EMT) inducer, TWIST1 was verified as a direct target gene of miR-539 through the application of a luciferase reporter assay. In conclusion, the results of the current study present evidence emphasizing the significance of the interactions between miR-539 and TWIST1 in the development of and progression of PC, highlighting its potential as a therapeutic target in the treatment of PC patients.

1. Introduction

Pancreatic cancer (PC) represents one of the most aggressive forms of cancer accompanied by a poor prognosis as well as a high mortality rate worldwide (Bray et al., 2018; Puleo et al., 2018; Wang et al., 2017). Although considerable advances in the arena of PC therapeutic methods have been made, the 5-year survival rate is still < 5% highlighting the need for further investigation into the potential molecular mechanisms associated with the condition (Canto et al., 2018; Li et al., 2011; Riquelme et al., 2018). Dysregulated microRNA (miRNA) profiles have been widely linked with the development of PC, suggesting the potential role of miRNAs as biomarkers and therapeutic targets in PC (Abreu et al., 2017; Frampton et al., 2015; Gibori et al., 2018; Karmakar et al., 2019; Ottaviani et al., 2018).

MiRNAs are a category of conservative noncoding short RNAs that

are 21–23 nucleotides lengthy (in mammals) (Qin et al., 2015). Binding to the 3′ untranslated region (3′-UTR) of target mRNAs has been reported to suppress translation or have a destabilizing effect on mRNAs along with the negative regulation of protein-coding genes (Yang et al., 2012). In regard to PC, many miRNAs have been implicated in the process of tumorigenesis, by influencing various cellular processes including proliferation, migration, and invasion. For instance, the over-expression of miR-221-3p has been reported to augment cell proliferation, while acting to inhibit apoptosis, whereas miR-1247 functions as a tumor suppressor in PC (Li et al., 2018; Yi et al., 2017). Recent discoveries demonstrated the pathogenesis of PC is associated with epithelial-mesenchymal transition (EMT) in a non-traditional manner, this perspective has provided major insight into the mechanism by which distant metastasis of various cancers occur highlighting the importance of identifying EMT-related miRNAs as

* Correspondence to: B. Pan, Department of Surgery, Wenzhou Central Hospital, The Dingli Clinical Institute of Wenzhou Medical University, No. 32, Dajian Lane, Wenzhou 325000, Zhejiang Province, PR China.

** Correspondence to: W. Ji, Research Institute of General Surgery, Nanjing School of Clinical Medicine, Southern Medical University (Nanjing General Hospital of Nanjing Military Region), No.1023, South Shatai Road, Baiyun District, Guangzhou 510515, Guangdong, China.

E-mail addresses: JiwuVIP@163.com (W. Ji), panbujianwz@163.com (B. Pan).

<https://doi.org/10.1016/j.yexmp.2019.04.012>

Received 24 September 2018; Received in revised form 25 March 2019; Accepted 19 April 2019

Available online 22 April 2019

0014-4800/ © 2019 Elsevier Inc. All rights reserved.

biomarkers or therapeutic targets (Guo, 2017).

Several studies reported a diminished expression of miR-539 in hepatocellular carcinoma (Zhu et al., 2016), osteosarcoma (Jin and Wang, 2015) as well as prostate cancer (Zhang et al., 2016), demonstrating its tumor suppressive capabilities. In 2015, Lv et al. asserted that miR-539 induces cell cycle arrest by aiming at cyclin-dependent kinase 4 in nasopharyngeal carcinoma (Lv et al., 2015). Gu et al. likewise recently concluded that miR-539 suppresses invasion and cell migration in thyroid cancer by aiming at CARMA1 directly (Gu and Sun, 2015). Additionally, further study has revealed that the over-expression of miR-539 could potentially at the very least inhibit PC cell invasion and EMT by targeting TWIST1, which is key EMT inducer. Nevertheless, the role and clinical significance of miR-539 in PC remains poorly understood. Thus, the central objective of the current study was to investigate the expression of miR-539 in clinical specimens and PC cell lines.

2. Materials and methods

2.1. Ethics statement

This study was conducted with the approval of the Ethical Committee of Wenzhou Central Hospital, The Dingli Clinical Institute of Wenzhou Medical University. All experiments were conducted in strict compliance with the Declaration of Helsinki. All participants signed informed consent documents. All animal experiments were approved by National Institutes of Health Animal Care and the Use Committee guidelines of the Wenzhou Medical University (Wenzhou, China).

2.2. Tissue samples and cell lines

A cohort of 52 PC samples and 52 corresponding adjacent normal pancreas tissues were collected from Wenzhou Central Hospital and Shanghai fengxian district central hospital between June 2011 and November 2016. The relevant basic clinical data is depicted in the Table 1. The samples from 52 patients with PC didn't were yet to undergo any form of radiotherapy or chemotherapy prior to surgery and stored at -80°C . Three PC cell lines (PANC-1, CFPAC-1 and BXP-3) and normal human pancreatic duct epithelial line (HPDE6-C7) were obtained from American Type Culture Collection (ATCC, VA, USA) and cultured in DMEM (Gibco, Grand Island, NY, USA) medium supplemented with fetal bovine serum (10%) (FBS; Invitrogen, Carlsbad, CA, USA) in 5% CO_2 cell culture incubator.

Table 1
Clinicopathological variables in 52 PC patients of this study.

Variable	Sample number (n)
Age	
≥ 60	37
< 60	15
Gender	
Male	33
Female	19
Lymphatic metastasis	
Yes	10
No	42
Differentiation level	
Low	12
High	40
Clinical stage	
I-II stage	39
III-IV stage	13

2.3. RNA isolation and real-time quantitative polymerase chain reaction (qRT-PCR)

RNAs were extracted using Trizol reagent (Invitrogen, Carlsbad, CA, USA). The TWIST1 mRNA expression levels were determined through the application of a gene-specific PCR primer synthesized by Shanghai GenePharma Company (Shanghai, China). Following primer confirmation, the expression of β -actin was regarded as an internal control in relation to the mRNA expression of TWIST1. The sequences of gene specific PCR primers were showed as follows (He et al., 2016): TWIST1, 5'-AGA AGT CTG CGG GCT GTG GCG-3' (forward), 5'-GAG GGC AGC GTG GGG ATG ATC-3' (reverse); E-cadherin: 5'-ACA ACG CCC CCA TAC CAG A-3' (forward) and 5'-CAC TCG CCC CGT GTG TTA GT-3' (reverse); N-cadherin: 5'-CTG AGC CTC ACC TGT GCG C-3' (forward) and 5'-CAC TCG CCC CGT GTG TTA GT-3' (reverse); Vimentin: 5'-AGCAT CTCCTCTGCAATTT-3' (forward) and 5'-AGGTGGACCAGCTAACCC AAC-3' (reverse); β -actin, 5'-AGT GTG ACG TGG ACA TCC GCA AAG-3' (forward) and 5'-ATC CAC ATC TGC TGG AAG GTG GAC-3' (reverse). U6 was regarded as a normalization reference in the process of miR-539 expression determination using TaqMan miRNA assays. The cells transfected with the delivery solutions served as the control group.

2.4. TWIST1 RNA interference

In order to knockdown TWIST1, the siRNAs (si-TWIST1, forward: 5'-GGU ACA UCG ACU UCC UCU AUU-3'; reverse: 5'-UAG AGG AAG UCG AUG UAC CUU-3') and negative control (si-NC, forward: 5'-UUC GAC UGU ACU CGA CAU CTT-3'; reverse: 5'-GAU GUC GAG UAC AGU CGA ATT-3') were purchased from GenePharma Company (Shanghai, China). PANC-1 and BXP-3 cells were transfected with si-TWIST1 or si-NC using Lipofectamine 2000 (Invitrogen, Carlsbad, CA, USA) according to the manufacturer's protocol. Cells transfected with the delivery solutions were served as the control group.

2.5. Plasmid construction

The TWIST1 coding sequence (forward primer: 5'-GAG ATG ATG CAG GAC GTG TC-3'; reverse primer: 5'-GTG GGA CGC GGA CAT GGA CCA-3') was inserted into pcDNA3.1 vector with an empty vector pcDNA3.1 as the control. The pre-miR-539 sequence (forward primer: 5'-CGT GAA TGA TAG TGA GGA AC-3'; reverse primer: 5'-GTG AAC GAT TTG CCA CAG ACA-3') was cloned into the PLKO.3G vector. Approximately 70% confluence cells were incubated and then a concentration of 2.0×10^5 TU lentiviruses was added into every well, which contained pre-miR-539 or a NC (GeneChem Company, Shanghai, China), and the expression levels of miR-539 were determined using qRT-PCR after infection for 7 days. Cells transfected with empty lentiviruses were served as the control group.

2.6. Cell proliferation, migration, and invasion assays

Proliferation ability was determined by the 3-(4, 5-dimethylthiazol-2-yl)-2, 5-diphenyltetrazolium bromide (MTT, Sigma, St Louis, MO, USA) assays as well as a clone formation assay. In brief, the cell lines were initially plated in 96-well plates (3000 per plate), following the addition of MTT solution (10 mg/mL) to each well which was subsequently assessed using a microplate reader at 570 nm. Meanwhile, a transwell invasion chamber coated with matrigel (Corning Glass Works, Corning, New York, USA) was used to determine the cell invasion ability, after which clone formation was utilized. The cells (5×10^4 /well) were plated in a 24-well plate. After 24 h had elapsed, the cells collected and seeded (1000–1500/well) in a fresh 6-well plate for a period of 14 days. Surviving colonies comprised of a minimum of 50 cells were record after being fixed with methanol/acetone (1:1) and stained with 5% crystal violet. According to the manufacturer's instructions, transwell invasion was measured with coated Matrigel. After

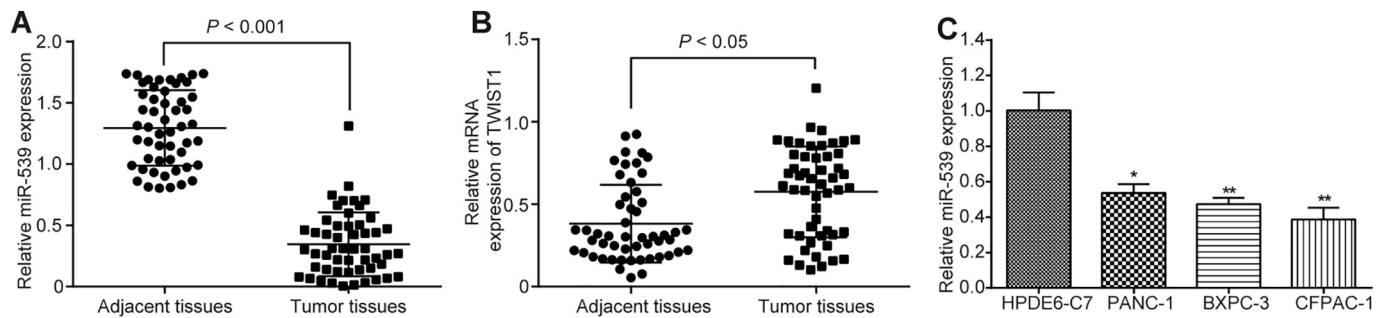


Fig. 1. miR-539 is significantly downregulated in PC tissues and cell lines and associated with an increased TWIST1 expression in the tissue specimen. The distribution of relative expression levels of miR-539 (A) and TWIST1 (B) in PC tumors (Tumor) and paired adjacent normal mucosa (Normal). (C) The relative expression level of miR-539 in PC cell lines and normal human pancreatic duct epithelial line HPDE6-C7. Measurement data are expressed as mean \pm standard deviation, and the experiments were repeated 3 times. * $P < .05$, ** $P < .01$, *** $P < .001$.

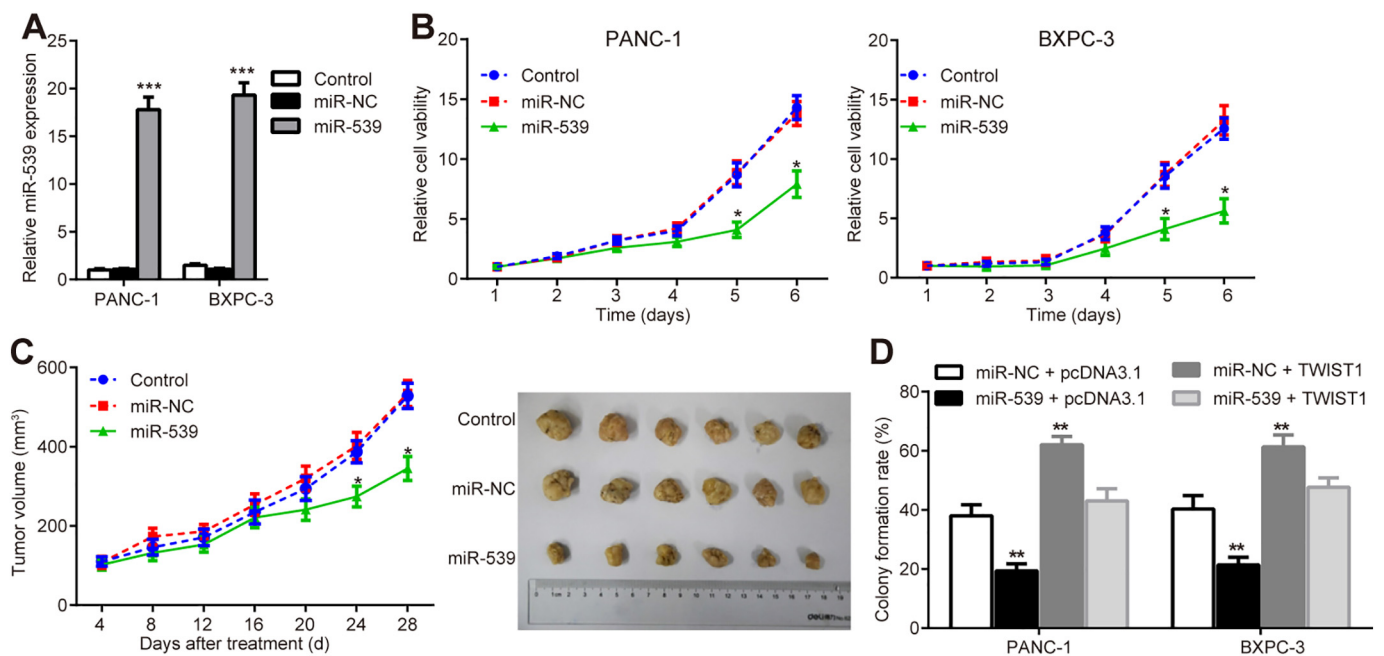


Fig. 2. miR-539 inhibits the proliferation of PC cells. (A) Ectopic expression of miR-539 in PC cell lines PANC-1 and BXPC-3 were evidence by qRT-PCR after transfection of miR-539. (B) miR-539 significantly inhibited PANC-1 and BXPC-3 cell viability. Cell growth rates were detected by MTT assay. (C) miR-539 inhibited PC cell growth in vivo. Tumor growth curve of miR-539 and control transfected PANC-1 cells in nude mice. (D) Colony formation assays in PANC-1 and BXPC-3 transfected with miR-NC or miR-539 with or without the TWIST1 expression plasmid. Measurement data are expressed as mean \pm standard deviation. Each group in A, B, D had 3 replicates while the groups in C had 6 replicates. * $P < .05$, *** $P < .001$.

fixed with 95% absolute alcohol, the cells invaded in the membrane then stained and counted. To further investigate the role of miR-539 in cell migration, we used wound healing assays to detect the ability. When the cells were cultured to approximately 90% confluence, wounds were scratched with pipette tips.

2.7. Luciferase activity assays

The interacting site between TWIST1 and miR-539 was predicted through RNA22 (<https://cm.jefferson.edu/rna22>). The wild-type (WT) 3'UTR of TWIST1 (forward primer: 5'-TCA GAG GAA CTA TAA GAA CAC CT-3'; reverse primer: 5'-CAA GCA GGT ATT TAC CAC CAA CT-3') was cloned to the downstream of the firefly luciferase gene in a pGL3-promoter vector. Scramble and miR-539 mimics as well as the corresponding inhibitors were purchased from Guangzhou RiboBio Co., Ltd. (China). The relative luciferase activity was conducted according to the manufacturers' instructions using a dual-luciferase assay kit (Promega, WI, USA). Cells transfected without miR-539 mimics were served the control group.

2.8. Western blot analysis

In order to determine the protein expression, approximately 30 mg/lane of protein was loaded and divided by 10% sodium dodecyl sulfate polyacrylamide gel electrophoresis (SDS-PAGE) followed by transfer onto a polyvinylidene fluoride membrane (Millipore Corporation, MA, USA). After blockade with 5% nonfat dry milk-TBS-0.1% Tween 20 for 2 h, the membranes were incubated with specific primary antibodies (all purchased from Cell Signaling Technology Inc., USA) against E-cadherin (1:1000 dilution; #14472S), Vimentin (1:1000 dilution; #5741S), N-cadherin (1:1000 dilution; #13116S), and β -actin (1:3000 dilution; #4970S) overnight at 4 °C followed by incubation with a horseradish peroxidase (HRP)-conjugated secondary antibodies (1:5000 dilution; Santa Cruz Biotechnology, Santa Cruz, CA). The abundance of target protein bands was densito-metrically determined using BandsScan 5.0 software, quantified, and presented as fold changes after normalization in accordance with the relevant invariant control.

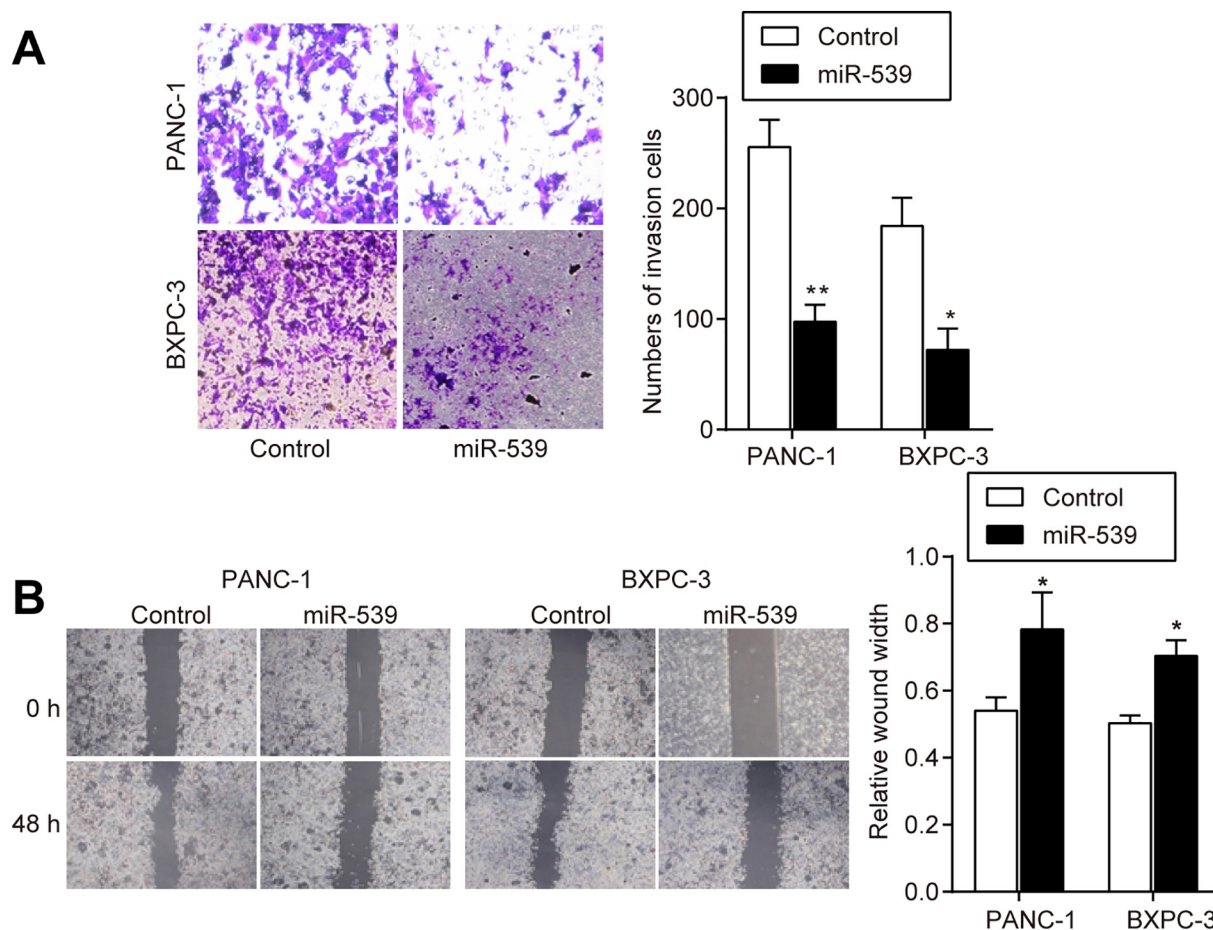


Fig. 3. miR-539 inhibits the invasion and migration of PC cells. (A) Transwell with matrigel assays was performed to investigate the invasion ability of PANC-1 and BXPC-3 cells. (B) Wound healing assays were performed to investigate the migration ability of PANC-1 and BXPC-3 cells. Measurement data are expressed as mean \pm standard deviation, and the experiments were repeated 3 times. * $P < .05$, ** $P < .01$.

2.9. In vivo tumor growth model

The in vivo tumor assay was performed with the transfection of PANC-1 cells (2×10^6) with miR-539 mimic or miR-NC, harvested, washed, re-suspended in serum-free RPMI-1640 medium, and injected into the left side of the posterior flank of the nude mice. Tumor growth rates were measured using Vernier calipers every 3 days until 28 days, and tumor volume (mm^3) was calculated using the following formula: volume = (length \times width²)/2. The volume of 6 tumors from each group was determined, with the mean value and the standard deviation subsequently plotted in Fig. 2. All mice were sacrificed after 28 days of inoculation. After stripping and weighing, parts of the tumor tissues were snap frozen in liquid nitrogen and stored at -80°C for further molecular detection.

2.10. Statistical analysis

All data were processed using SPSS 21.0 statistical software (IBM Corp, Armonk, NY, USA). Normal distribution and variance homogeneity were tested for all the data. The measurement data with normal distribution were expressed as mean \pm standard deviation. The independent *t*-test was used for comparison between two groups. Multi-group comparisons were conducted using one-way analysis of variance, followed by the Tukey's post hoc test. Differences were considered significant if $P < .05$.

3. Results

3.1. MiR-539 is down-regulated in PC tissues and cells and associated with an increased Twist expression in the tissue specimen

As illustrated in Fig. 1A, the miR-539 expression, which was determined by qRT-PCR, was substantially diminished in the PC tissues in comparison with that of the paired adjacent normal pancreas tissue. The expression of Twist in the tissue specimen was determined, which revealed a significant increase in the expression of the PC tissues when compared to the paired adjacent normal pancreas tissue (Fig. 1B). Moreover, our results revealed that miR-539 expression in PC cell lines were considerably lower than that of the normal human pancreatic duct epithelial line HPDE6-C7 (Fig. 1C). Taken together, the observed outcomes suggest that depleted miR-539 expression may be related with PC carcinogenesis.

3.2. MiR-539 inhibits the proliferation, invasion, and migration of PC cells

In an attempt to identify the functional role of miR-539 in PC cells, lentiviral vector expressing miR-539 was constructed and used to infect BXPC-3 cells and PANC-1. Next, qRT-PCR revealed that miR-539 overexpression was validated (Fig. 2A). Additionally, MTT assay results illustrated that miR-539 compared with the transfection with an empty vector (Fig. 2B). To further assess the impact of miR-539 on PC growth in vivo, PANC-1 cells were transfected with miR-539 or miR-NC were injected into mouse, with tumor volume determined every 3 days until the mice were executed. As displayed in Fig. 2C, tumor growth of the

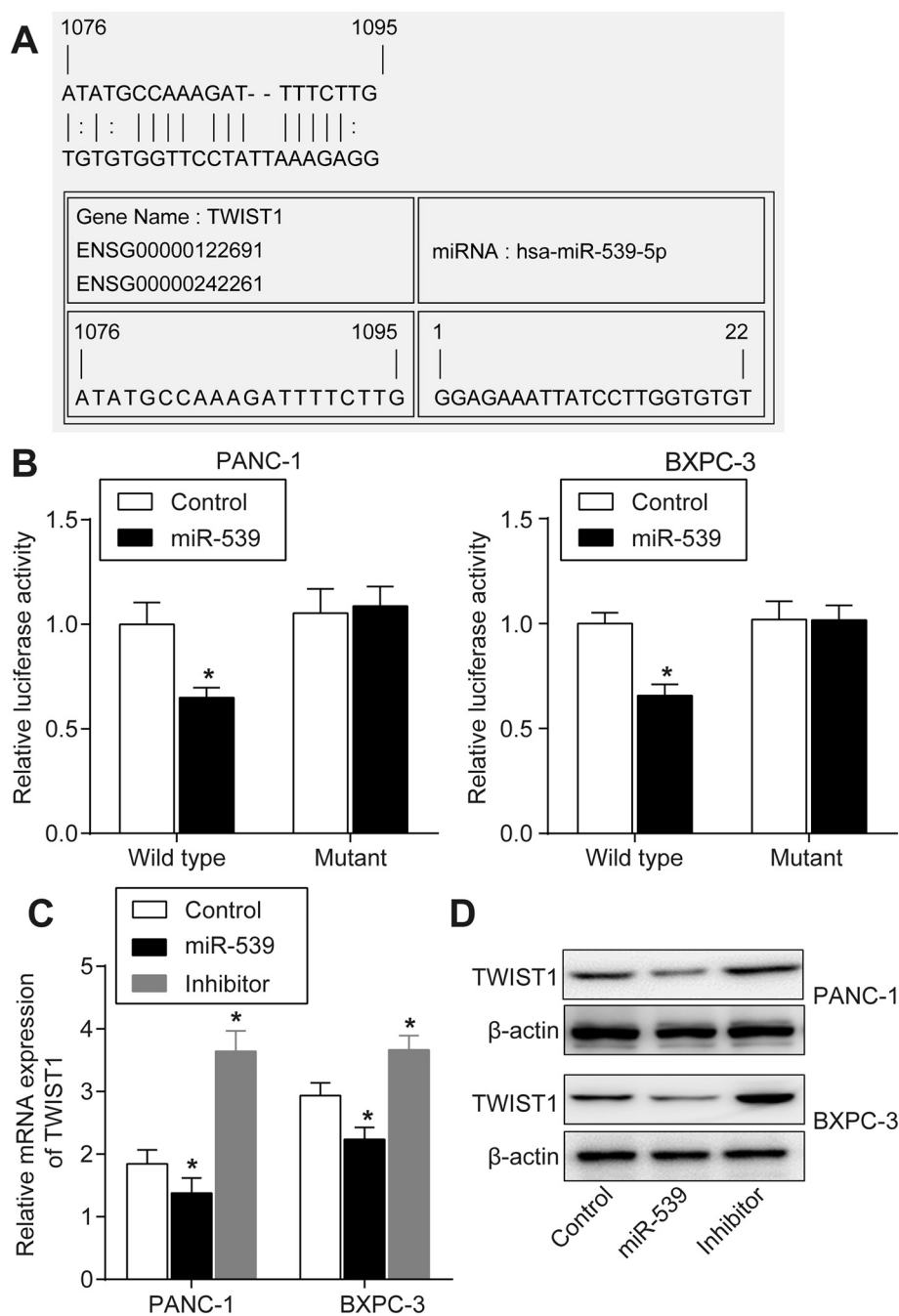


Fig. 4. miR-539 directly inhibits TWIST1 by targeting its 3'UTR. (A) The miR-539 binding site predicted in the TWIST1 3'UTR. (B) Mutant TWIST1 3'UTR was generated at the seed region as indicated by the underline. A fragment of TWIST1 3'UTR containing wild type (WT) or mutant (Mut) of the miR-539 binding sites was cloned to the downstream of the luciferase reporter gene vector, then PANC-1 and BXPC-3 cells were transfected with reporter vectors containing either wild-type or mutant TWIST1 3'UTR with either miR-539 mimics (miR-539) or scrambled mimics as negative control (miR-NC). Luciferase activity was determined 48 h after transfection. (C) TWIST1 mRNA expression levels were detected by qRT-PCR in PANC-1 and BXPC-3 cells transfected with miR-539 mimics (miR-539) or miR-539 inhibitor mimics (inhibitor). The untreated cells were taken as control. (D) TWIST1 protein expression level was detected by Western blot analysis in PANC-1 and BXPC-3 cells transfected with miR-539 mimics (miR-539) or miR-539 inhibitor mimics (inhibitor). Measurement data are expressed as mean ± standard deviation, and the experiments were repeated 3 times. **P* < .05.

miR-539 overexpressing group was smaller than that of the control group and miR-NC. Meanwhile, the overexpression of TWIST1 was found to be able to rescue the miR-539 for the process of cell proliferation (Fig. 2D). Moreover, from the outcome of transwell matrigel assays (Fig. 3A), and wound healing assays (Fig. 3B), we identified that miR-539 overexpression suppressed the cell invasion and migration capability of BXPC-3 cells and PANC-1 considerably.

3.3. TWIST1 is a direct target gene of miR-539

In order to examine the possible target of miR-539, we predicted the binding sites between TWIST1 and miR-539 through a bioinformatics website RNA22 (<https://cm.jefferson.edu/rna22/>). TWIST1 possesses a putative binding site of miR-539, as illustrated in Fig. 4A. In order to ascertain as to whether miR-539 targets TWIST1 3'UTR in an instant manner, luciferase reporter assay was executed in BXPC-3 cells and

PANC-1, the results of which suggested that miR-539 mimics scaled down the luciferase while this diminished activity was not detected in the TWIST1 3'UTR reporter with mutant miR-539 binding seed sites (Fig. 4B). Furthermore, Western blot analysis and qRT-PCR methods also demonstrated that miR-539 mimics simulated the diminution of TWIST1 expression, while elevated expression of TWIST1 was simulated by miR-539 inhibitor mimics in BXPC-3 cells and PANC-1 (Fig. 4C, D). In conclusion, our results demonstrated that miR-539 suppresses the expression of TWIST1 instantly in PC cells.

3.4. MiR-539's inhibitory effects are attenuated by TWIST1 in relation to the epithelial-mesenchymal transition (EMT) of PC cells

Additionally, as an important inducer of EMT, TWIST1 plays a vital role in migration and cell invasion, so we focused on TWIST1 in this research. As illustrated in Fig. 5A, B, the transfection efficiency of

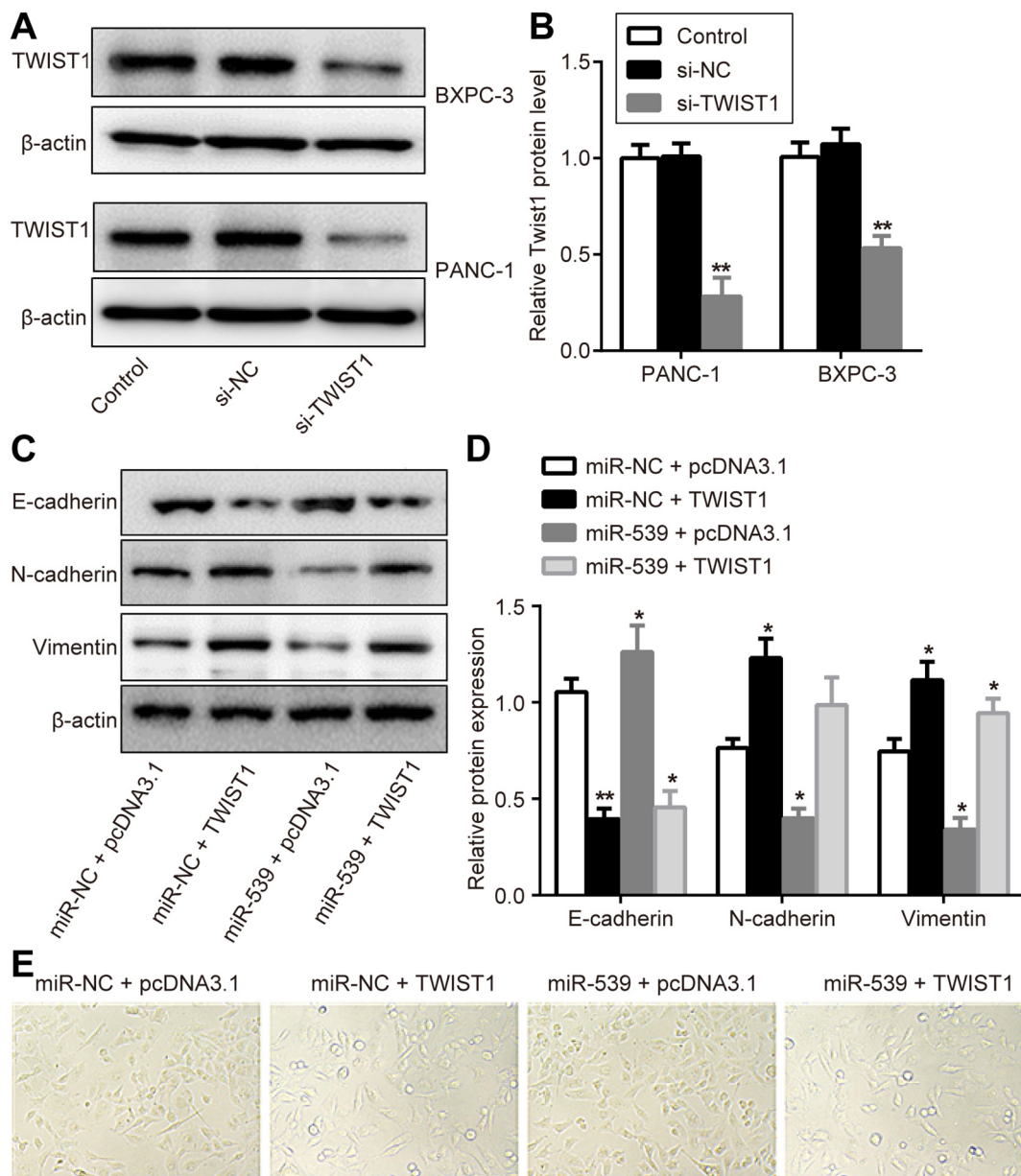


Fig. 5. TWIST1 attenuates the inhibitory effects of miR-539 on EMT of PC cells. (A, B) PANC-1 and BXPC-3 cells were transfected with TWIST1-specific small interfering RNA (si-TWIST1) or negative control (si-NC), and knockdown of TWIST1 was validated by Western blot analysis. (C, D) Western blot analysis was performed to examine the effects of miR-539 overexpression only (miR-539 + pcDNA3.1), rescued TWIST1 only (miR-NC + TWIST1), combined miR-539 overexpression with rescued TWIST1 (miR-539 + TWIST1), and negative control (miR-NC + pcDNA3.1) on EMT markers (E-cadherin, N-cadherin, and Vimentin) in PANC-1 cells. (E) Observation of cell morphology. Measurement data are presented as mean ± standard deviation, and the experiments were repeated 3 times. **P* < .05, ***P* < .01.

specific siRNA knockdown of TWIST1 in PANC-1 and BXPC-3 cells were determined accordingly. Moreover, in order to further examine the function of miR-539 and TWIST1 in EMT, we detected that TWIST1 could attenuate miR-539's inhibitory influences considerably on the inhibition of EMT in PANC-1 cells (Fig. 5C, D) in connection with the TWIST1 rescue experimentations. The overexpression of miR-539 was found to increase the expression of epithelial marker (E-cadherin) while simultaneously suppressed the levels of mesenchymal markers (Vimentin and N-cadherin). The results of morphological examination showed that compared with the miR-NC + pcDNA3.1 treatment, cells following miR-539 + pcDNA3.1 were in elongated spindle shape, the majority of which were accompanied by formation of long filamentous pseudopod, while the miR-NC + TWIST1-treated cells was in ovoid, with close connection between cell membranes (Fig. 5E). Taken

together, the observations of the experiment exhibited that TWIST1 attenuates the miR-539 inhibitory effects on PC cells' EMT, which was further confirmed through the results obtained in the examination of cell morphology.

4. Discussion

PC remains a challenging and aggressive cancer, accompanied with a high rate of mortality (Inamdar et al., 2016; Regine et al., 2008; Xiao et al., 2016). The molecular pathogenesis and mechanism of PC progression at present, are yet to be fully elucidated. Accumulating evidence has indicated that the dysregulation of miRNA is a convoluted process associated with the progression of various human tumors (Li et al., 2015; Schultz et al., 2014). In the present study, we examined the

descended expression of miR-539 in a cohort of three PC cell lines and 52 PC patients. Meanwhile, increased expression of miR-539 inhibited invasion, EMT process and PC cell proliferation were detected. TWIST1 was determined to be a direct target gene of miR-539 based on the results of the luciferase reporter assay in the PC cell. Key data revealed that miR-539 potentially operates as a tumor suppressor in PC cells. TWIST1, as a basic-helix-loop-helix family transcription factor, has been reported to play a vital role in heaps of pathological diseases' process (Bulzico et al., 2017).

Accumulating studies have recently indicated that TWIST1 regulates tumor metastasis by influencing (EMT, which is a crucial process for metastasis and cancer invasion (Xu and Zhang, 2017). TWIST1 activation is significant enough to promote EMT and the dissemination of tumor cells, while the overexpression of TWIST1 has been correlated with a more sinister prognosis and aggressive cancer strains (Tao et al., 2017). The hypoxic status can induce EMT process of tumor cells via activating TWIST1. TWIST1 overexpression plays a significant role in regulating cancer initiation, progression and metastasis in a variety of regulatory pathways (Xiong et al., 2017). Therefore, targeted therapy aiming at TWIST1 represents a promising therapeutic target for PC therapy. During the current study, viaRNA22 (<https://cm.jefferson.edu/rna22/>), the prediction of the TWIST1 gene as a possible target gene of miR-539 was executed. Luciferase reporter assays provided evidence demonstrating that TWIST1 is a direct miR-539 target. Meanwhile, the results from qRT-PCR and western blot analysis confirmed the miR-539 could inhibit the TWIST1 expression in PANC-1 and BXP-3 cells (Fig. 4C, D). The results revealed that TWIST1 mRNA effectively acts as an efficient miR-539 sponge. The level of miR-539 was elevated after we silenced the TWIST1 expression (Fig. 5A, B). Afterwards, further investigation into the functional role of miR-539's in PC cell lines was conducted, which comprised of expressing BXP-3 cells and PANC-1. MTT, transwell with matrigel, and wound healing assays. The results obtained illustrated that miR-539 could suppress cell proliferation, invasion, migration, and EMT through TWIST1 in BXP-3 cells and PANC-1.

Taken together, our results indicated that TWIST1 is a functional target of miR-539 in PC cells. Additionally, miR-539 was substantially down-regulated in PC, suggesting that miR-539 might be a modulator of EMT. Additionally, miR-539 increased various epithelial marker such as E-cadherin, while acting to suppress mesenchymal markers such as N-cadherin and Vimentin.

5. Conclusions

To conclude, the prevailing findings illustrated that miR-539 is downregulated in cell lines and PC samples and suppresses migration and invasion of PC cells by targeting TWIST1. The key findings of the current study present evidence indicating that the tumor-suppressive activity of miR-539 is associated with the augmentation of the expression of epithelial marker (E-cadherin) and inhibition of mesenchymal markers (N-cadherin and Vimentin) by targeting TWIST1. The restoration of miR-539 may consequently serve as a potential therapeutic strategy for PC treatment.

Conflicts of interest

The authors have no conflict of interest to report.

Acknowledgements

This work was supported by the following foundations: Medical and Health Science and Technology Plan Project of Zhejiang Province (No. 2018RC066); The experimental animal science and technology plan project of Zhejiang province (No. 2018C37110).

References

- Abreu, F.B., Liu, X., Tsongalis, G.J., 2017. miRNA analysis in pancreatic cancer: the Dartmouth experience. *Clin. Chem. Lab. Med.* 55, 755–762.
- Bray, F., Ferlay, J., Soerjomataram, I., et al., 2018. Global cancer statistics 2018: GLOBOCAN estimates of incidence and mortality worldwide for 36 cancers in 185 countries. *CA Cancer J. Clin.* 68, 394–424.
- Bulzico, D., Torres, D.C., Ferreira, G.M., et al., 2017. A novel TP53 mutation associated with TWIST1 and SIP1 expression in an aggressive adrenocortical carcinoma. *Endocr. Pathol.* 28, 326–331.
- Canto, M.I., Almario, J.A., Schulick, R.D., et al., 2018. Risk of neoplastic progression in individuals at high risk for pancreatic cancer undergoing long-term surveillance. *Gastroenterology* 155, 740–751 e742.
- Frampton, A.E., Castellano, L., Colombo, T., et al., 2015. Integrated molecular analysis to investigate the role of microRNAs in pancreatic tumour growth and progression. *Lancet* 385, S37 Suppl 1.
- Gibori, H., Eliyahu, S., Krivitsky, A., et al., 2018. Amphiphilic nanocarrier-induced modulation of PLK1 and miR-34a leads to improved therapeutic response in pancreatic cancer. *Nat. Commun.* 9, 16.
- Gu, L., Sun, W., 2015. MiR-539 inhibits thyroid cancer cell migration and invasion by directly targeting CARMA1. *Biochem. Biophys. Res. Commun.* 464, 1128–1133.
- Guo, Q., 2017. Changes in mitochondrial function during EMT induced by TGFbeta-1 in pancreatic cancer. *Oncol. Lett.* 13, 1575–1580.
- He, X., Wei, Y., Wang, Y., et al., 2016. MiR-381 functions as a tumor suppressor in colorectal cancer by targeting Twist1. *Onco Targets Ther.* 9, 1231–1239.
- Inamdar, S., Slattery, E., Bhalla, R., et al., 2016. Comparison of adverse events for endoscopic vs percutaneous biliary drainage in the treatment of malignant biliary tract obstruction in an inpatient national cohort. *JAMA Oncol.* 2, 112–117.
- Jin, H., Wang, W., 2015. MicroRNA-539 suppresses osteosarcoma cell invasion and migration in vitro and targeting Matrix metalloproteinase-8. *Int. J. Clin. Exp. Pathol.* 8, 8075–8082.
- Karmakar, S., Kaushik, G., Nimmakayala, R., et al., 2019. MicroRNA regulation of K-Ras in pancreatic cancer and opportunities for therapeutic intervention. *Semin. Cancer Biol.* 54, 63–71.
- Li, L.S., Bey, E.A., Dong, Y., et al., 2011. Modulating endogenous NQO1 levels identifies key regulatory mechanisms of action of beta-lapachone for pancreatic cancer therapy. *Clin. Cancer Res.* 17, 275–285.
- Li, L., Li, B., Chen, D., et al., 2015. miR-139 and miR-200c regulate pancreatic cancer endothelial cell migration and angiogenesis. *Oncol. Rep.* 34, 51–58.
- Li, F., Xu, J.W., Wang, L., et al., 2018. MicroRNA-221-3p is up-regulated and serves as a potential biomarker in pancreatic cancer. *Artif. Cells Nanomed. Biotechnol.* 46, 482–487.
- Lv, L.Y., Wang, Y.Z., Zhang, Q., et al., 2015. miR-539 induces cell cycle arrest in nasopharyngeal carcinoma by targeting cyclin-dependent kinase 4. *Cell Biochem. Funct.* 33, 534–540.
- Ottaviani, S., Stebbing, J., Frampton, A.E., et al., 2018. TGF-beta induces miR-100 and miR-125b but blocks let-7a through LIN28B controlling PDAC progression. *Nat. Commun.* 9, 1845.
- Puleo, F., Nicolle, R., Blum, Y., et al., 2018. Stratification of pancreatic ductal adenocarcinomas based on tumor and microenvironment features. *Gastroenterology* 155 (1999-2013 e1993).
- Qin, C.Z., Lou, X.Y., Lv, Q.L., et al., 2015. MicroRNA-184 acts as a potential diagnostic and prognostic marker in epithelial ovarian cancer and regulates cell proliferation, apoptosis and inflammation. *Pharmazie* 70, 668–673.
- Regine, W.F., Winter, K.A., Abrams, R.A., et al., 2008. Fluorouracil vs gemcitabine chemotherapy before and after fluorouracil-based chemoradiation following resection of pancreatic adenocarcinoma: a randomized controlled trial. *JAMA* 299, 1019–1026.
- Riquelme, E., Maitra, A., McAllister, F., 2018. Immunotherapy for pancreatic Cancer: more than just a gut feeling. *Cancer Discov.* 8, 386–388.
- Schultz, N.A., Dehendorf, C., Jensen, B.V., et al., 2014. MicroRNA biomarkers in whole blood for detection of pancreatic cancer. *JAMA* 311, 392–404.
- Tao, Y., Han, T., Zhang, T., et al., 2017. LncRNA CHRFR-induced miR-489 loss promotes metastasis of colorectal cancer via TWIST1/EMT signaling pathway. *Oncotarget* 8, 36410–36422.
- Wang, J., Zhang, Y., Wei, H., et al., 2017. The mir-675-5p regulates the progression and development of pancreatic cancer via the UBQLN1-ZEB1-mir200 axis. *Oncotarget* 8, 24978–24987.
- Xiao, A.Y., Tan, M.L., Wu, L.M., et al., 2016. Global incidence and mortality of pancreatic diseases: a systematic review, meta-analysis, and meta-regression of population-based cohort studies. *Lancet Gastroenterol. Hepatol.* 1, 45–55.
- Xiong, H., Nie, X., Zou, Y., et al., 2017. Twist1 enhances hypoxia induced Radioresistance in cervical Cancer cells by promoting nuclear EGFR localization. *J. Cancer* 8, 345–353.
- Xu, F., Zhang, J., 2017. Long non-coding RNA HOTAIR functions as miRNA sponge to promote the epithelial to mesenchymal transition in esophageal cancer. *Biomed. Pharmacother.* 90, 888–896.
- Yang, X., Yu, J., Yin, J., et al., 2012. MiR-195 regulates cell apoptosis of human hepatocellular carcinoma cells by targeting LATS2. *Pharmazie* 67, 645–651.
- Yi, J.M., Kang, E.J., Kwon, H.M., et al., 2017. Epigenetically altered miR-1247 functions as a tumor suppressor in pancreatic cancer. *Oncotarget* 8, 26600–26612.
- Zhang, H., Li, S., Yang, X., et al., 2016. miR-539 inhibits prostate cancer progression by directly targeting SPAG5. *J. Exp. Clin. Cancer Res.* 35, 60.
- Zhu, C., Zhou, R., Zhou, Q., et al., 2016. microRNA-539 suppresses tumor growth and tumorigenesis and overcomes arsenic trioxide resistance in hepatocellular carcinoma. *Life Sci.* 166, 34–40.